G&G 2011

BROWNISH RED ZIRCON FROM MULING, CHINA

Tao Chen, Hao Ai, Mingxing Yang, Shu Zheng, and Yungui Liu

Gem-quality brownish red zircon occurs in alluvium derived from Tertiary alkali basalt at Muling in the northeast Chinese province of Heilongjiang. Rough and cut samples were characterized using standard gemological methods, electron microprobe, LA-ICP-MS, and Raman and UV-Vis-NIR spectroscopy. Internal features consisted of melt inclusions, apatite, magnetite, fluid inclusions, and color zones. The samples contained abundant rare-earth elements, but showed only slight radiation damage and properties consistent with "high" zircon. Although it has yet to be mined commercially, the Muling deposit is a promising source of gem zircon.

Zircon ($ZrSiO_4$) is a common accessory mineral, occurring in a wide variety of sedimentary, igneous, and metamorphic rocks (Finch and Hanchar, 2003). Often appearing as small, rounded grains, zircon also can form large (up to a centimeter or more), well-formed prismatic crystals. Zircon has long been used as a gem material because of its high dispersion and relatively high refractive index (Faulkner and Shigley, 1989). Major sources of gem zircon are Sri Lanka, Madagascar, Cambodia, and Tanzania (Shigley et al., 2010). The present study provides a detailed characterization of brownish red zircon from Muling, China (e.g., figure 1).

LOCATION AND GEOLOGIC BACKGROUND

Muling is a city of more than 300,000 in the northeastern Chinese province of Heilongjiang (figure 2). It lies in the mid-northern section of the Dunhua-Mishan fault, which forms the northern branch of the Tanlu fault (Qiu et al., 2007). Zircon is known from three main deposits within the city limits—at Gangouzi, Fusheng, and Hanchangou—where it occurs in alluvium derived from weathered Tertiary alkali basalt. The gems have been recovered from areas measuring up to 1700 m long and 20–200 m wide, at depths of 0.3–1.2 m. Associated heavy minerals in the alluvium include yellow, blue, pink, and colorless sapphire; garnet; and spinel (with some of these three in gem quality); enstatite, olivine, and chromite also occur. All of these minerals were probably originally transported to the earth's surface as megacrysts in the alkali basalt. U-Pb age dating indicates the zircon has a crystallization age of 9.39 ± 0.4 million years.

The Muling deposits were discovered in 1985, but mining is still limited. So far, it has consisted of informal surface digging by local people, who extract the gems by hand after washing the alluvial material. Zircon is more common than corundum, and it has been recovered as a byproduct of sapphire mining. The commercial potential of the deposits has not been evaluated, nor have the source rocks for the gems been located.

MATERIALS AND METHODS

The materials examined were either recovered on site by author HA or purchased from local miners. The samples consisted of 17 rough pieces, 3 faceted stones, and 23 polished plates (~1 mm thick). Most of the plates were cut in specific orientations—that is, parallel (11 plates) or perpendicular (10 plates) to the c-axis. The rough zircons ranged from 4 × 2 × 2 mm to 17 × 6 × 5 mm, and the faceted stones weighed 0.40–1.33 ct (see, e.g., figure 3). Refractive indices on small crushed fragments (<0.5 mm) derived from five pieces of rough were measured using immersion oil

See end of article for About the Authors and Acknowledgments.
GEMS & GEMOLOGY, Vol. 47, No. 1, pp. 36–41.

Figure 1. Muling, in northeastern China, is the source of these brownish red zircons (1.90–3.33 ct). Photo by Robert Weldon.

and the Becke line method. Other standard gemological properties (pleochroism, SG, fluorescence, and absorption spectrum with the hand spectroscope) were obtained from the rough samples and nine of the polished plates. All of the polished plates were observed for microscopic features.

Chemical composition was measured on five of the polished plates (cut from four samples). Major elements were analyzed by electron microprobe using a JEOL JXA-8100 instrument. The analyzed elements included Mg, Ca, Mn, Al, Zr, Fe, Si, and Hf. Trace-element concentrations, including rare-earth elements (REE), were measured by laser ablation–inductively coupled plasma–mass spectrometry (LA-ICP-MS). Laser sampling was performed using a MicroLas Geolas 2005 system equipped with a 193 nm ArF-excimer laser. Helium was selected as the carrier gas to enhance transport efficiency of the ablated material. Argon was used as the makeup gas and mixed with the carrier gas before entering the ICP. An Agilent 7500a ICP-MS was utilized to acquire ion-signal intensities. Sampling pits had a

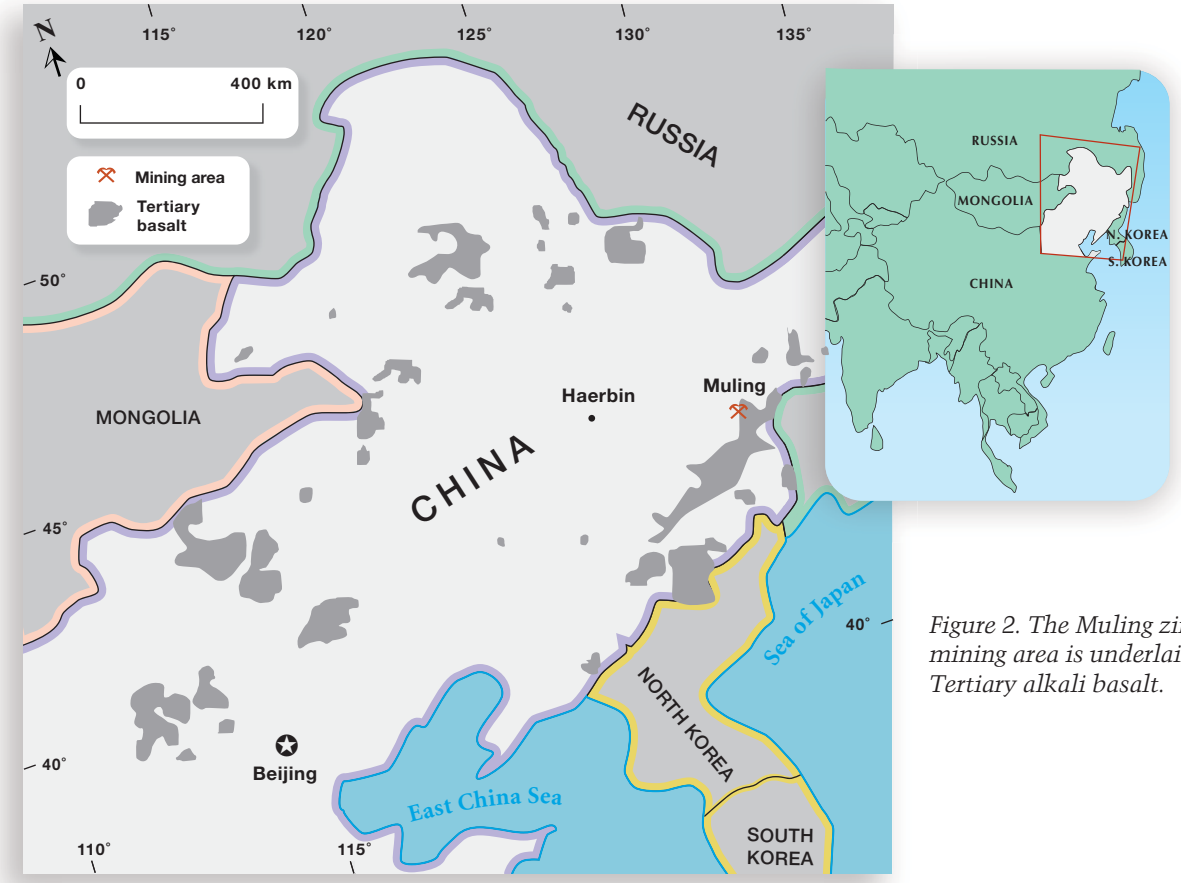

Figure 2. The Muling zircon mining area is underlain by Tertiary alkali basalt.

Figure 3. These rough (left, 0.07–0.84 g) and faceted (right, 0.40–1.33 ct) zircons are some of the samples examined for this report. Photos by T. Chen.

diameter of about 60 μm. Each analysis included an approximately 20 second background acquisition followed by 50 seconds of data acquisition. Calibration was performed using NIST SRM 610 glass as an external standard in conjunction with internal calibration using Si following the methods of Longerich et al. (1996) and Günther et al. (1999). The SRM 610 standard was selected because it contains concentrations of certain elements that are close to those in the zircon samples of this study. Analyses of USGS rock standards (BIR-1G and BHVO-2G) indicated that the precision (1σ, relative standard deviation) was better than 10% for trace elements.

Raman spectra of the zircon and its inclusions were recorded with a Renishaw MKI-1000 spectrometer coupled to an argon-ion laser (514.5 nm). In each experiment, three scans were collected and averaged. Polarized UV-Vis-NIR absorption spectra were measured using a Shimadzu UV-1601 spectrophotometer in the 200–800 nm range, with a step interval of 0.5 nm and scan speed of 2.64 nm/second. Both types of spectra were recorded from nine oriented polished plates.

Three reddish brown and two dark brownish red zircon crystals were chosen for heat treatment experiments. Heating was carried out in air using a YFX 9/13Q-YC furnace. The samples were placed in quartz sand in a corundum crucible and heated from room temperature to 1100°C at a rate of 5°C/minute. After annealing at the target temperature for 24 hours, the samples were cooled for 6 hours. The furnace door was opened slightly when the temperature cooled to about 150°C, and the samples were removed at approximately room temperature.

RESULTS AND DISCUSSION

Gemological Properties. The crystals showed a combination of tetragonal prismatic and pyramidal faces. The samples ranged from red to brownish red, and were generally transparent to translucent with some cracks. Their refractive indices (>1.81) and specific gravity values (4.57–4.69) were consistent with "high" zircon (e.g., O'Donoghue, 2006). The hand spectroscope showed no absorption features except for faint lines below 600 nm in some samples; no characteristic absorption lines in the red region were noted.

Melt inclusions were common, occurring individually and in groups. These inclusions were captured during crystal formation and record the conditions present during their growth. Glass melt inclusions formed dark ovoids, as seen previously in zircon by Thomas et al. (2003). Some melt inclusions, ranging from ~10 to 50 μm, consisted of metamict zircon surrounded by a decrepitation halo; each metamict zircon typically contained one or two internal voids (figure 4). Two apatite inclusions were observed, one a short semitransparent crystal and the other a long colorless transparent prism (figure 5). A group of dark brownish red crystals in one sample (figure 6) were identified as magnetite. Parallel color zones, fractures, and fluid inclusions also were observed in some samples.

NEED TO KNOW

- Brownish red zircon is produced as a byproduct of artisanal mining for basalt-derived sapphires at Muling in northeastern China.
- The zircon is only slightly metamict, with properties that are consistent with "high" zircon.
- The brownish red coloration is due to radiation damage, and the stones can be lightened by heating in air.

Chemical Composition. Trace-element signatures in igneous zircons are linked to their source-rock type and crystallization environment. Table 1 lists the

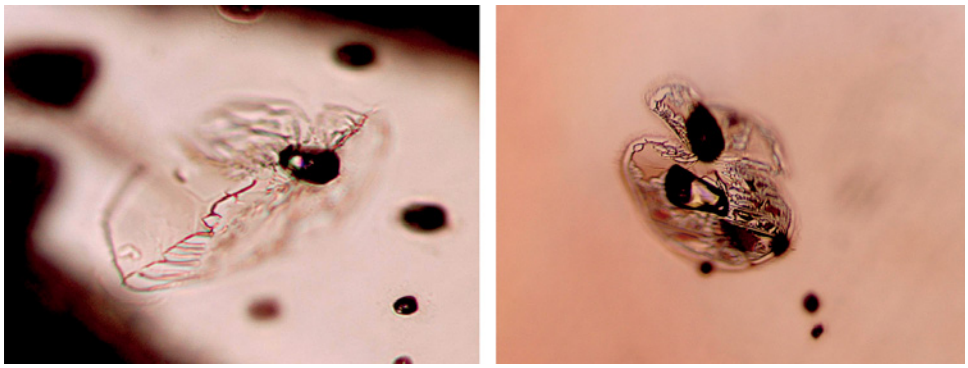

Figure 4. Metamict zircon inclusions in the zircon samples often contain one or two voids and have halos of small decrepitated melt inclusions surrounding them. Photomicrographs by T. Chen; magnified 200× (left) and 100× (right).

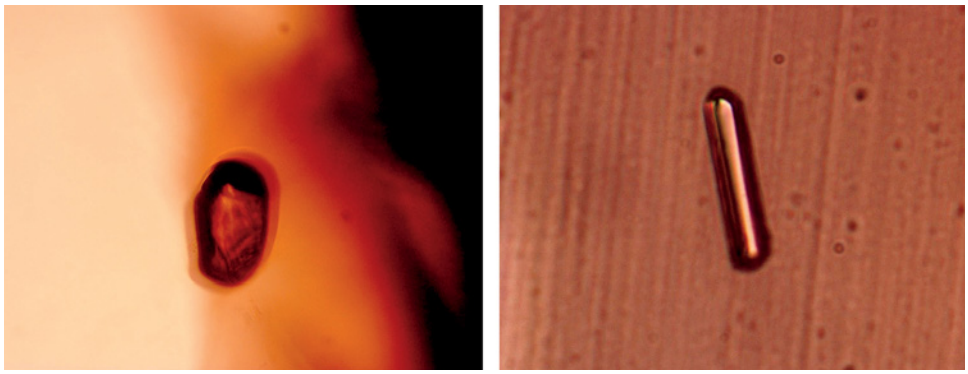

Figure 5. Apatite inclusions were observed as high-relief stubby crystals (left, 66 μm long) and colorless prisms (right, 110 μm long). Photomicrographs by T. Chen.

major- and trace-element composition of four zircons from Muling. The predominant impurities were Hf, Al, Mg, Ca, Y, REE, P, Th, and U. The concentrations of Th (355–2440 ppm) and U (341–871 ppm) were high enough that they would be expected to cause metamictization of zircon over time. The relatively high concentration of rare-earth elements (again, see table 1) indicates that the Muling zircons came from mafic rocks (Fan et al., 1998).

Raman Spectroscopy. Figure 7 shows the polarized Raman spectra of four representative samples of Muling zircon. Some of the main features include the internal modes at 1005 cm^{-1} (Si–O ν_3 stretching), 973 cm^{-1} (Si–O ν_1 stretching), and 438 cm^{-1} (Si–O ν_2 bending). The assignments of the bands at 393 and 356 cm^{-1} are still the subject of debate, and have been described as internal or external modes. The three bands at 224, 213, and 201 cm^{-1} are generally considered lattice modes, such as vibrations involving SiO_4 tetrahedrons and Zr ions (Hoskin and Rodgers, 1996; Nasdala et al., 2003). The reason for variations in the relative intensity of the most prominent bands at 1005 and 356 cm^{-1} has not yet been well explained.

Nasdala et al. (1998) showed that Raman spectra of slightly to moderately metamict zircons have the same band pattern as crystalline zircon; however, the full width at half maximum (FWHM) of the intense mode at about 1000 cm^{-1} increases as a function of radiation damage (Nasdala et al., 1998). In well-crystallized zircon, the ν_3 FWHM is less than 5 cm^{-1}, while partially metamict zircon commonly has a FWHM value greater than 10 cm^{-1}. In this study, ν_3 FWHM values ranged from 5.15 to 5.56 cm^{-1}, indicating well-crystallized material (i.e.,

Figure 6. This group of magnetite inclusions in zircon occurred as short, parallel prisms. Photomicrograph by T. Chen; magnified 200×.

TABLE 1. Major- and trace-element composition of four samples of zircon from Muling, China.[a]

Composition	C-1	C-2	C-4	P-4	P-10
Oxide (wt.%)					
SiO_2	33.82	33.15	33.03	32.79	32.92
ZrO_2	62.30	64.32	63.88	63.63	64.62
HfO_2	1.21	1.20	1.10	1.19	1.11
Al_2O_3	0.04	0.05	0.03	0.06	0.07
MgO	0.03	0.04	0.02	0.03	0.03
CaO	0.03	0.03	0.03	nd[b]	0.02
Total	97.43	98.79	98.09	97.70	98.77
Element (ppmw)					
La	0.014	0.016	0.100	0.045	0.051
Ce	75.9	113	334	203	247
Pr	0.19	0.27	1.34	0.90	0.95
Nd	3.64	5.33	21.5	13.9	15.9
Sm	9.53	13.3	35.1	24.8	27.5
Eu	5.44	7.50	16.6	12.3	14.6
Gd	58.6	81.8	139	109	126
Tb	22.3	30.8	41.4	33.9	39.5
Dy	265	363	403	351	401
Ho	95.5	129	123	109	126
Er	390	519	438	401	465
Tm	78.4	99.6	78.2	73.4	83.1
Yb	641	809	586	567	642
Lu	107	137	90.1	85.9	105
REE (total)	1752	2309	2307	1985	2294
P	367	376	234	201	240
Ti	2.67	3.15	8.55	5.06	8.51
Y	2752	3687	3347	2972	3552
Nb	13.4	19.5	67.5	30.3	57.4
Hf	7463	7458	7218	7005	7667
Ta	3.89	5.36	13.6	7.90	13.7
Pb	0.600	0.740	2.22	0.840	1.52
Th	355	487	2440	613	1373
U	341	404	871	439	679

[a] *"C" represents a sample cut perpendicular to the c-axis, and "P" represents a sample cut parallel to the c-axis. The number following the letter refers to the sample number (i.e., C-4 and P-4 were polished plates cut from the same rough zircon).*
[b] *Abbreviation: nd = not detected. Elements not detectable in all samples are not shown in the table.*

"high" zircon). The FWHM value of ν_3 measured from the zircon inclusions (figure 4) was 9.47 cm^{-1}, indicating they were partially metamict.

UV-Vis-NIR Spectroscopy. Zircon coloration depends on transition metal content and the presence of radiation-induced color centers (Nasdala et al., 2003). Polarized UV-Vis-NIR absorption spectra from one sample are shown in figure 8. The spectra are similar to that of a brownish red zircon from Chanthaburi, Thailand, which is believed to be colored by radiation damage (see minerals.caltech.edu/files/visible/zircon/index.htm). The characteristic absorption spectra, consisting of sharp lines below 600 nm, are attributed

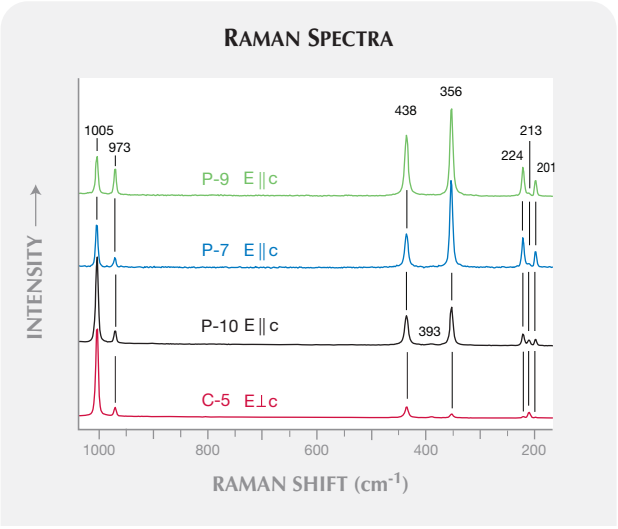

Figure 7. Polarized Raman spectra of oriented polished plates of Muling zircon show different relative band intensities. The most intense band in samples C-5 and P-10 is at 1005 cm^{-1}, whereas the strongest band in P-7 and P-9 is at 356 cm^{-1}.

to f-f transitions (movement of electrons between atomic f orbitals of different energies) related to REEs and elements such as U and Th (actinides and lanthanides). As in most natural zircon, these sharp lines are weak and faint (Nasdala et al., 2003).

Heat Treatment. Figure 9 shows five zircons before (top) and after (bottom) heating to 1100°C. After the experiment, their tone significantly lightened and

Figure 8. These polarized UV-Vis-NIR absorption spectra were obtained from two polished plates (~1 mm thick) cut from the same crystal.

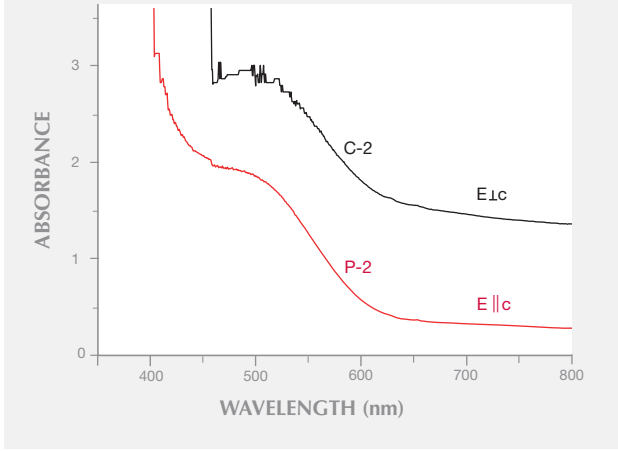

much of the red hue was removed. The color changes seemed to be less related to the original hue than to the amount of inclusions in the sample; heating caused the more transparent zircons to become more colorless. However, some orange areas were seen around cracks in the heated samples. We expect that more commercially desirable colors can be obtained by heating for shorter durations and/or at lower temperatures.

CONCLUSION

Alluvial deposits at Muling, in northeastern China, host gem-quality brownish red zircon crystals that show a combination of tetragonal prismatic and pyramidal faces. Melt inclusions are common, and trace-element content indicates a mafic source. Raman spectroscopy suggests they underwent very little radiation damage. Polarized UV-Vis-NIR absorption spectra showed weak sharp lines caused by f-f transitions related to actinides and lanthanides. This locality shows potential as a commercial source of gem zircon.

Figure 9. These Muling zircon samples (0.49–0.77 g), shown before and after heating, became significantly lighter after heat treatment. Photos by Y. Liu.

ABOUT THE AUTHORS

Dr. Chen (summerjewelry@163.com) is a research scientist, Dr. Yang is a gemologist and dean, and Mr. Liu is a graduate student at the Gemmological Institute, China University of Geosciences, Wuhan. Mr. Ai is a graduate student at the State Key Laboratory of Ore Deposit Geochemistry, Chinese Academy of Sciences, Guiyang. Mr. Zheng is a researcher at the State Key Laboratory of Geological Processes and Mineral Resources, China University of Geosciences, Wuhan.

ACKNOWLEDGMENTS

This research was supported by the National Natural Science Foundation of China and by the outstanding young teacher fund from the China University of Geosciences.

REFERENCES

Fan A.N., Liu R.X., Li H.M., Li N., Sui J.L., Lin Z.R. (1998) Zircon chronology and REE geochemistry of granulite xenolith at Hannuoba. *Chinese Science Bulletin*, Vol. 43, No. 18, pp. 1510–1515.

Faulkner M.J., Shigley J.E. (1989) Zircon from the Harts Range, Northern Territory, Australia. *G&G*, Vol. 25, No. 4, pp. 207–215.

Finch R.J., Hanchar J.M. (2003) Structure and chemistry of zircon and zircon-group minerals. In J.M. Hanchar, Ed., *Zircon, Reviews in Mineralogy and Geochemistry*, Vol. 53, Mineralogical Society of America and Geochemical Society, Washington, DC, pp. 1–25.

Hoskin P.W.O., Rodgers K.A. (1996) Raman spectral shift in the isomorphous series $(Zr_{1-x}Hf_x)SiO_4$. *European Journal of Solid State and Inorganic Chemistry*, Vol. 33, pp. 1111–1121.

Longerich H.P., Jackson S.E., Günther D. (1996) Inter-laboratory note. Laser ablation inductively coupled plasma mass spectrometric transient signal data acquisition and analyte concentration calculation. *Journal of Analytical Atomic Spectrometry*, Vol. 11, pp. 899–904.

Nasdala L., Pidgeon R.T., Wolf D., Irmer G. (1998) Metamictization and U-Pb isotopic discordance in single zircons: A combined Raman microprobe and SHRIMP ion probe study. *Mineralogy and Petrology*, Vol. 62, pp. 1–27.

Nasdala L., Zhang M., Kempe U., Panczer G., Gaft M., Andrut M., Plöze M. (2003) Spectroscopic methods applied to zircon. In J.M. Hanchar, Ed., *Zircon, Reviews in Mineralogy and Geochemistry*, Vol. 53, Mineralogical Society of America and Geochemical Society, Washington, DC, pp. 427–466.

O'Donoghue M., Ed. (2006) *Gems*, 6th ed. Butterworth-Heinemann, Oxford, UK.

Qiu Z.L., Yany J.H., Yang Y.H., Yang S.F., Li C.Y., Wang Y.J., Lin W.P., Yang XX. (2007) Trace element and hafnium isotopes of Cenozoic basalt-related zircon megacrysts at Muling, Heilongjiang Province, northeast China. *Acta Petrologica Sinica*, Vol. 23, No. 2, pp. 481–492.

Shigley J.E., Laurs B.M., Janse A.J.A., Elen S., Dirlam D.M. (2010) Gem localities of the 2000s. *G&G*, Vol. 46, No. 3, pp. 188–216.

Thomas J.B., Bodnar R.J., Shimizu N., Chesner C.A. (2003) Melt inclusions in zircon. In J.M. Hanchar, Ed., *Zircon, Reviews in Mineralogy and Geochemistry*, Vol. 53, Mineralogical Society of America and Geochemical Society, Washington, DC, pp. 63–87.